Physical Layer of a Novel Broadband Low-Level Fieldbus with Discrete Multitone

Thomas Handte, Matthias Breuninger, Hanns Thilo Hagmeyer, and Joachim Speidel
Institute of Telecommunications, University of Stuttgart
Pfaffenwaldring 47
70569 Stuttgart, Germany
{handte, breuninger, hagmeyer, speidel}@inue.uni-stuttgart.de

Abstract

We present the physical layer for a broadband low-level fieldbus for industrial applications. Using discrete multitone (DMT) in combination with adaptive modulation, the system is able to deal with arbitrary network topologies as well as with narrowband interferers. Moreover, it can serve a multitude of users with high and user-specific data rates at a very low bit error probability. First, we outline the channel characteristics, and show that DMT provides a highly flexible modulation scheme for such network topologies. We then describe the system concept and provide a block diagram of the transceiver. Additionally, a frame structure is introduced and analyzed regarding all relevant parameters.

1. Introduction

In the last years, the need for higher data rates to be transmitted in low-level fieldbus networks has continuously increased. In typical applications only a few bits were transferred between a central data collection unit (master) and various sensors or actuators (slaves), because only rather simple devices had to be addressed, e.g. simple on/off-switches. In the future, more intelligent devices will communicate a larger amount of data. However, the cycle time which is the round-trip time of a message between a master and a slave should be kept in the order of a few milliseconds or even lower in order to fulfill the requirements imposed by process and factory automatization. Additionally, more and more sensors are placed within a factory plant, which increases the amount of slaves and the lengths of the transmission lines. Typically, such networks should be very flexible in the sense that they can support different numbers of slaves in arbitrary positions on the transmission lines (multidrop feature) and up to 128 or even more slaves should be supported, simultaneously. Although, such systems operate in the very harsh industrial field where heavy distortion arising from impulse noise and sinusoidal interferers is present, they have to provide a very good transmission quality and though a very low bit error ratio (BER).

Due to the stringent requirements mentioned above, current low-level fieldbus systems like [1] are forced to operate at their performance edge. Their data throughput can only be increased slightly because a higher clock rate of line coded signals, e.g. Manchester code would result in a strong intersymbol interference (ISI) due to symbol overlapping. Consequently, the symbol error probability and hence the retransmission rate (RTR) for erroneously received messages would rise unacceptably. Thus, new communication concepts based on advanced modulation and coding techniques are essentially required.

We present a novel system concept for a low-level fieldbus which can provide a high flexibility regarding multidrop applications, scalability, and slave specific data rates. Our concept features discrete multitone (DMT) which divides the transmission bandwith into narrowband subcarriers. They are allocated individually to every slave depending on both the actual position within the network and the desired data rate. In contrast to today's low-level fieldbus systems, our scheme replaces serial communication and offers parallel access to all slaves. Thereby, the data of each slave is separated by different subcarrier frequencies which are mutually orthogonal to each other. By applying time division duplex, an almost bidirectional and real-time communication can be achieved. A forward error correction (FEC) safeguards the bits to be transmitted and assures a very low BER of less than 10^{-9}.

The paper is organized as follows: In Section 2 we describe the system by addressing the channel conditions in 2.1. We introduce the modulation scheme in 2.2, and a block diagram of the transceiver in 2.3. The frame structure is presented in 2.4, and Section 3 concludes the paper.

2 System Description

2.1 Channel Characteristics

In the following, we discuss the broadband channel characteristics arising in arbitrary network topologies. In this regard, we compute the transfer function of a rather simple wireline network shown in Fig. 1. The network consists of three subscribers, namely one master and two slaves, which communicate bidirectionally with the mas-

978-1-4673-0692-8/12/$31.00 ©2012 IEEE

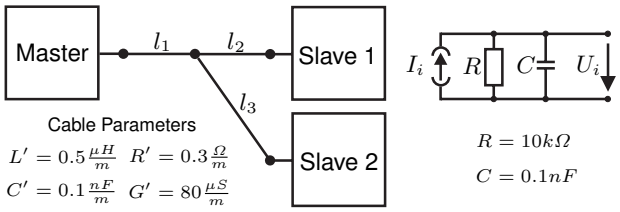

Figure 1. Simple exemplary network setup.

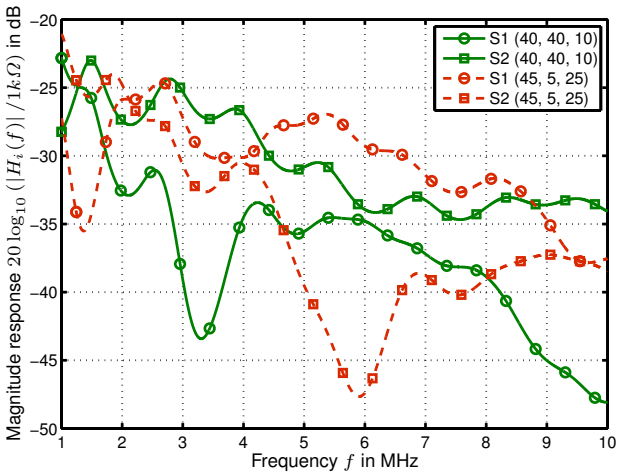

Figure 2. Magnitude response from master to slave 1 (S1) and slave 2 (S2) for various cable lengths (l_1, l_2, l_3) in meters.

ter. The cable parameters are given in Fig. 1, as well as the equivalent output circuit of a subscriber. In the downlink, when the master transmits data to slave i, the transfer function is given by

$$H_i(f) = \frac{U_i(f)}{I_0}, \tag{1}$$

where U_i is the received voltage of slave i as a function of the frequency f and I_0 denotes the transmit current of the master. Figure 2 shows the absolute value of the transfer functions, namely the magnitude responses in the frequency range from 1 MHz up to 10 MHz for different cable lengths (l_1, l_2, l_3) in meters. We see that the magnitude responses are frequency-selective caused by signal reflexions at the connection node and the subscribers, since their impedances are not matched to the cable parameters. Because of the decreasing input impedance of a subscriber, $|H_i(f)|$ tends to decrease at higher frequencies. In practical networks this effect is even enforced because of the skin effect which raises $R' \sim \sqrt{f}$ and which was neglected here. Clearly, signals coming from slaves which are located far away from the master suffer a greater attenuation than signals coming from closer slaves, which can be clearly observed in the $(40, 40, 10)$-setup.

This illustrates that broadband fieldbus systems operating with arbitrary network topologies must be able to cope with various frequency-selective channel scenarios which can be even time-variant in case that network sections are changed during operation. Please note that the exemplary network shown in Fig. 1 is a rather simple network setup and that the frequency-selectivity of the magnitude response is even enforced when more sophisticated topologies are considered.

2.2 Discrete Multitone

In this section, we briefly introduce DMT which is especially designed for the afore mentioned channel conditions. DMT represents the real baseband version of orthogonal frequency division multiplexing (OFDM) which is used for wireless communications. Basically, DMT divides the total transmission bandwith into N narrowband subcarriers which can be independently modulated by symbols coming from a phase-shift keying (PSK) constellation, for example. The time-domain signal is formed at the transmitter side by an inverse fast Fourier transform (IFFT) of size $2N$ which combines N complex symbols to a set of $2N$ real-valued signal samples which is referred to as a DMT symbol. If subcarrier k is modulated by the complex symbol $a_k^R + ja_k^I$, a DMT symbol is given by [2]

$$x(n) = \sqrt{\frac{2}{N}} \sum_{k=1}^{N-1} a_k^R \cos\left(\frac{\pi}{N} nk\right) - a_k^I \sin\left(\frac{\pi}{N} nk\right) \tag{2}$$

where we dropped data transmission at DC ($k = 0$).

Obviously, the N subcarriers are uniformly distributed over the transmission bandwith f_g, hence two adjacent subcarriers have a frequency spacing of $\Delta f = \frac{f_g}{N}$. The real-valued signal samples of a DMT symbol are then transformed into analog domain by a digital-to-analog converter (DAC) with sampling frequency f_a. Thus, the maximum transmission bandwidth is fixed to $f_g = \frac{f_a}{2}$. At the receiver side, the inverse operations are performed in order to retrieve the transmitted symbols. A detailed discussion on DMT is given in [2] and the references therein.

Using DMT in frequency-selective channels has major advantages compared to other transmission techniques. First of all, it is robust against ISI when a guard interval (GI) is used. A GI is introduced in the transmit signal and it consists of a cyclic repetition of the last N_g samples of the DMT symbol as follows:

$$\underbrace{x(2N - N_g), \ldots, x(2N-1)}_{\text{guard interval}}, \underbrace{x(0), \ldots, x(2N-1)}_{\text{DMT symbol}}$$

Thus, a DMT symbol with GI has a length of $2N + N_g$ signal samples, which clearly lowers the spectral efficiency by a factor of $\frac{2N}{2N+N_g}$. However, at the receiver side, ISI is completely removed as long as the maximum delay-spread arising from the channel or timing misalignments is smaller than the duration of the GI given by $\frac{N_g}{f_a}$.

Due to the fact that the bandwidth is divided into independent subcarriers, the communication scheme can adapt itself to the actual channel conditions. Subcarriers with an insufficient quality are not used, whereas others are considered for data transmission. The quality of a subcarrier

is measured individually by means of the signal-to-noise ratio (SNR) which has to be estimated at the receiver side and which has to be forwarded to the master in order to perform a subcarrier allocation to the slaves. If we assume frequency-flat noise, for example, the SNR has the frequency-selective characteristics of the squared magnitude responses in Fig. 2. There, one can also observe that if the $(45, 5, 25)$-setup is considered, a subcarrier at $f = 6$ MHz is indeed of poor quality for slave 2, whereas it would be rather good for slave 1. In this case, the master would allocate the subcarrier at $f = 6$ MHz to slave 1, while another subcarrier would be considered for slave 2.

Additionally, the system is also quite flexible to individual data rates which can be easily augmented by allocating several subcarriers to a slave. However, the increase in data rate is subjected to the current channel conditions, since they limit the maximum throughput and as every subcarrier can only be allocated once, the number of slaves within the network is limited then.

Although DMT offers various advantages as outlined before, it also requires an accurate synchronization in both time and sampling frequency alignment [3] which has to be assured by dedicated algorithms.

The subcarriers can in principle be modulated individually. Clearly, the higher the modulation order gets, the more bits can be transmitted per time interval. However, the requirements regarding subcarrier quality increase simultaneously, if the BER should be kept below a given target. In order to limit the overall complexity of our system, we propose that a subcarrier is either modulated by no symbol in the case of a bad SNR or by differential quadrature phase shift keying (DQPSK) which maps two bits to four different phase values. In this case, the symbol set is given by $\left\{0, \exp(j0), \exp(-j\frac{\pi}{2}), \exp(j\pi), \exp(j\frac{\pi}{2})\right\}$.

For a differential modulation, the actual information is transmitted in the phase difference of two symbols [4]. The differential modulator computes the actual phase value $\varphi_{k,l}$ of subcarrier k at point in time l such that the receiver can retrieve the correct information when building the difference $\Delta\varphi_k = \varphi_{k,l} - \varphi_{k,l-1}$. Clearly, since the difference is calculated regarding time index l, an initialization phase value $\varphi_{k,0}$ has to be provided, which is transmitted by means of a DMT reference symbol. When using differential modulation, a phase shift coming from the channel does not affect the signal constellation, since this effect is canceled out when computing $\Delta\varphi_k$. Thus, pilots and estimation algorithms for the channel phase can be avoided at the expense of a SNR loss of about 3 dB [4].

For safeguarding the bits to be transmitted, a FEC is applied to the information bits before they are mapped to DQPSK symbols. The proposed scheme uses a shortened BCH-code in order to keep the block length and cycle time small. This code can correct up to 3 bit errors and at the receiver side a quality indicator is additionally computed which gives a measure of the decision reliability. In case that the decision was not reliable enough, the code word is dropped and requested again. On the details of this advanced error detection strategy, we refer to [5], where also an in-depth discussion on the achievable BER and RTR is provided. Using this code for $K_c = 20$ information bit to be transmitted which yields $N_c = 38$ bit including redundancy, one can achieve a BER of 10^{-12} with an average RTR of 10^{-3} at an SNR of approximately 11 dB.

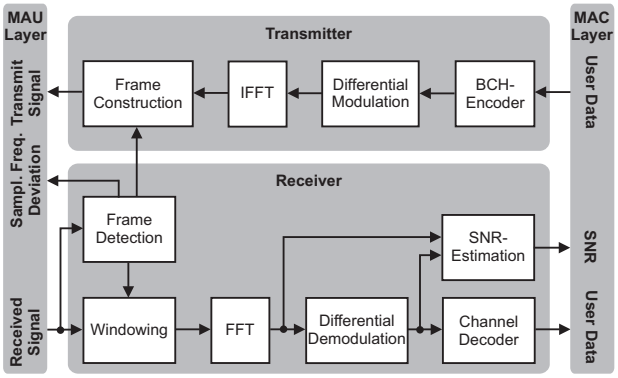

Figure 3. Block diagram of modulation layer.

2.3 Block Diagram of the Transceiver

Figure 3 depicts a simplified block diagram of the modulation sublayer (MDS) which provides interfaces to the medium attachment unit (MAU) and the medium access control layer (MAC). The MAU provides the circuitry for bus connection as well as analog-to-digital converter (ADC), DAC, amplifiers, and filters. On the other hand, the MAC [6] provides algorithms for network management like subcarrier allocation, for example.

At the transmitter side, the user data is first encoded by a BCH-encoder. Then these bits are differentially mapped to symbols and are passed on to an IFFT which generates the time-domain signal. Within the frame construction, the transmission frame is built up and the transmit frame is aligned properly to the received signal.

At the receiver side, a windowing function extracts the DMT symbols by discarding the GI. Consequently, the receiver has to know the symbol timing which is provided by the frame detection when operating as slave. The extracted DMT symbols are then passed to a fast Fourier transform (FFT) which transforms the received signal into frequency domain. On every subcarrier, differential demodulation is performed in order to retrieve the bits which are then processed by the channel decoder. The received data is then passed to the MAC if the transmission was reliable enough, otherwise retransmission is requested. Moreover, a SNR estimation algorithm observes the quality of a subcarrier and provides this data to the MAC.

The MDS of master and slave differ only in the frame detection which is exclusively used for a slave, while the master sets the frame structure on its time basis as a reference for all salves. Consequently, a slave provides a control signal for sampling clock correction which can be exploited by a controllable oscillator within the MAU.

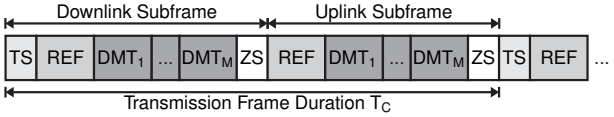

Figure 4. Frame structure.

2.4 Frame Structure

In the following, we illustrate the structure of the transmission frame shown in Fig. 4. Every frame starts with the downlink subframe, where data is transferred from the master to the slaves. The downlink subframe is built up of a training sequence (TS), a DMT reference symbol (REF), M DMT data symbols with GI and a zero symbol (ZS). Subsequently, an uplink subframe follows, in which data is transferred from the slaves to the master. This subframe is built up similarly to the downlink subframe except of the TS which is not sent in uplink. Note that in downlink only the master transmitter is active, whereas in the uplink case all slave transmitters are enabled, each sending on its individually allocated subcarrier(s). Thus, the uplink signal is a superposition of the signals coming from all slaves. The TS consists of a dedicated sequence of length N_{TS} which is used for synchronization [1]. The DMT reference symbol in combination with the data symbols contain coded user data and during a ZS of length N_Z a transmit break is provided so that the MAU can switch between transmit and receive mode. Since all mentioned signal samples need to be transmitted within the cycle time T_C

$$N_{TS} + 2N_Z + 2(M+1)(2N + N_g) = T_C f_a \qquad (3)$$

holds. The data rate η per modulated subcarrier measured at the MAC interface in down- and uplink is then given by

$$\eta = \frac{2MK_c}{T_C N_c}, \qquad (4)$$

as two bit per subcarrier and DMT symbol are transmitted.

These equations have to be evaluated under certain boundary conditions. The limit on N_g is given by the round-trip delay that a signal suffers when traveling to the subscriber which is located most far away from the master and back. If the longest distance is defined as l_{max} and the lowest propagation velocity in the considered frequency range is given by v_{min},

$$\frac{N_g}{f_a} > \frac{2l_{max}}{v_{min}} \qquad (5)$$

holds. The limits of f_g and consequently of f_a heavily depend on the cable characteristics, noise and impedance parameters of the MAU. Moreover, implementation costs increase simultaneously with f_a, since the ADC, DAC and the digital circuits need to support higher sampling rates.

Table 1 evaluates the eqs. (3) to (5) for typical parameters. Here, we considered the BCH-code of Sec. 2.2,

[1] The TS is not sent in uplink, since in a multiuser scenario both TS signal design and detection would be very complex in implementation. However, synchronization in downlink only is usually sufficient.

Table 1. Exemplary parameter sets.

N	T_C[ms]	$\eta[\frac{\text{kbit}}{\text{s}}]$	N_g	f_a[MHz]	l_{max}[m]
128	1	20	99	15	< 462
256	1.68	11.9	99	15	< 462

where on every subcarrier $K_c = 20$ bit can be transmitted, which yields to $M = 19$ with redundancy. Additionally, $N_{TS} = 160$ and $N_Z = 320$ holds and for f_a and N_g as given in Tab. 1, eq. (3) yields T_C. Considering the cable parameters of Fig. 1, v_{min} amounts to $1.4{\cdot}10^8$ $\frac{\text{m}}{\text{s}}$ and l_{max} can readily be computed according to eq. (5). Finally, eq. (4) gives the achievable data rate η per subcarrier.

Table 1 and eq. (3) clearly show that if N is doubled more samples have to be transmitted and consequently T_C increases as f_a stays constant. However, T_C does not increase linearly, since the relative loss in spectral efficiency introduced by the GI tends to zero as N increases.

3 Conclusion

We have presented the physical layer of a broadband low-level fieldbus system which can provide high and scalable data rates for arbitrary network topologies. First, we outlined the channel characteristics of such networks and provided an adaptive modulation scheme which can deal with frequency selective channels. Besides the basic principles, a block diagram of the modulation layer and a frame structure were presented and analyzed. We illustrated the performance of our scheme which can offer an increase in data rate of several orders when compared to today's low-level fieldbus systems. Additionally, it achieves a cycle time of a few milliseconds and maximum network lengths of several hundred meters.

Acknowledgment

This work was funded by the German Federal Ministry of Economics and Technology (BMWi 16IN0672).

References

[1] "Low-voltage switchgear and controlgear - Controller-device interfaces (CDIs) - Part 2", 2008, IEC 62026-2.

[2] R. Schur, S. Pfletschinger, and J. Speidel, "DMT Modulation", in J. G. Proakis, editor, *Wiley Encyclopedia of Telecommunications*, volume 2, pp. 736–748. Wiley and Sons, 2003.

[3] T. Pollet and M. Peeters, "Synchronization with DMT Modulation", *IEEE Commun. Mag.*, vol. 37, no. 4, pp. 80–86, Apr. 1999.

[4] R. van Nee and R. Prasad, *OFDM for Wireless Multimedia Communications*, Artech House, 2000.

[5] M. Breuninger and J. Speidel, "Performance of Combined Error Correction and Error Detection for very Short Block Length Codes", accepted for IEEE Int. Symp. on Ind. Electron., May 2012.

[6] M. Voss, K.-P. Kirchner, A. Fink, and H. Beikirch, "Packet-Based Time-Critical Medium Access for a Process-Oriented Deterministic Bus System", to appear, 2012.